Supporting information:

Synthesis of large-area high quality 2D BiOI single crystal for highly sensitive ultraviolet photodetection

Yixiang Li [a], Zhipeng Fu [a], Bicheng Wang[b], Yu Yao [a, b], Jiashuai Yuan[b], Meng Li [b], Xu He[, b], Wei Liu [*, b]*

[a] College of Chemistry, Fuzhou University, Fuzhou 350108, PR China CAS Key

[b] CAS Key Laboratory of Design and Assembly of Functional Nanostructures, and Fujian Provincial Key Laboratory of Materials and Techniques toward Hydrogen Energy, Fujian Institute of Research on the Structure of Matter, Chinese Academy of Sciences, Fuzhou, Fujian, 350002, PR China

E-mail: hexu@fjirsm.ac.cn, liuw@fjirsm.ac.cn

The spatial restriction growth mechanism:

In the growth process of space-confined molten salt method, the BiI_3 power dissolves into the liquid phase and then crystallizes by reaction with oxygen into ultra-thin two-dimensional sheets above the melting point, the space limitation is conducive to the growth of ultra-thin crystals.

Detailed calculation methods for UV-visible absorption spectra：

The UV-visible absorption spectra of the sample were obtained from the equation:

$$A_{BiOI} = A_{BiOI\,+\,Mica} - A_{Mica}$$

Where A_{BiOI} is the absorption of BiOI nanosheets, $A_{BiOI+Mica}$ is the absorption of both the BiOI nanosheets and mica substrate, and A_{Mica} is the absorption of bare mica substrate. The $A_{BiOI+Mica}$ and A_{Mica} were obtained by the UV-VIS absorption spectrum test.

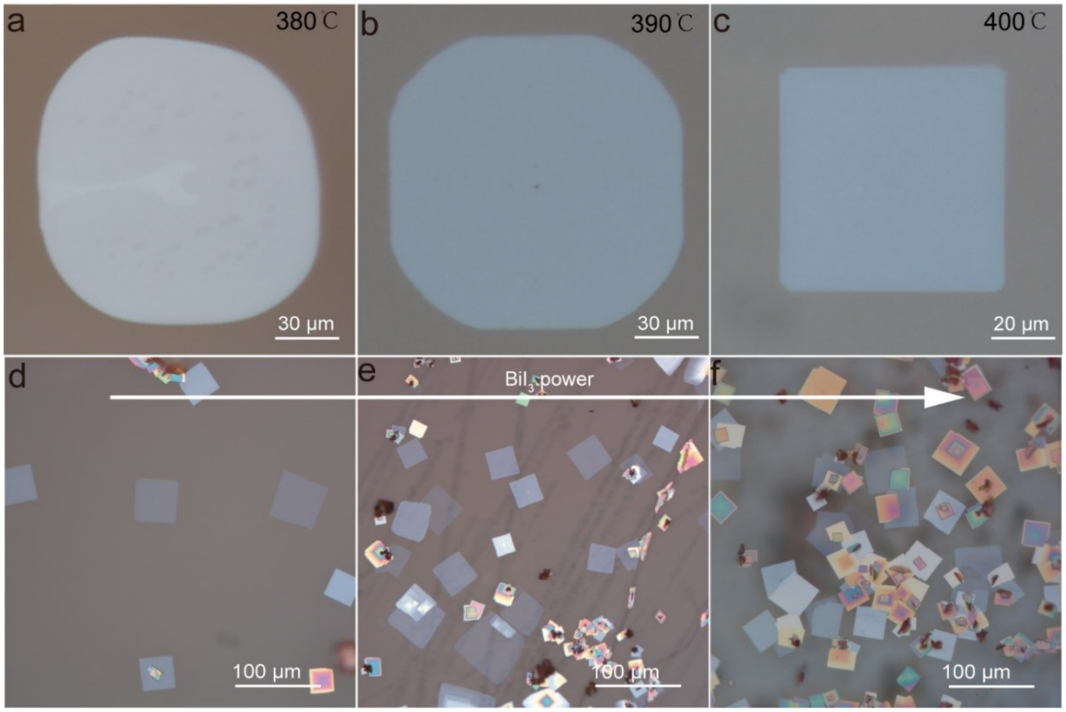

Figure S1. Growth regulation of BiOI nanosheets on mica. (a, b, c) BiOI nanosheets with different morphologies were grown at 380 ℃, 390 ℃ and 400 ℃. (d, e, f) Different morphologies of BiOI nanosheets grown from low to high BiI_3 concentrations.

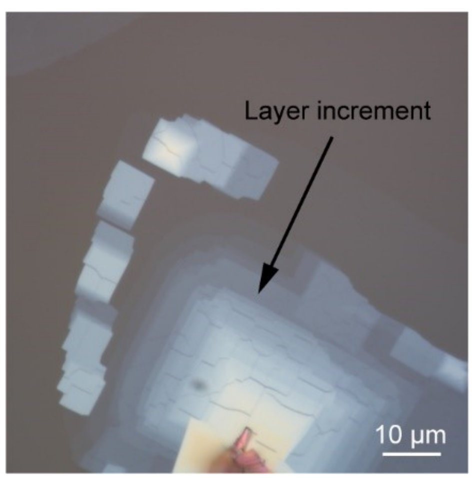

Figure S2. Layered BiOI optical images for Raman testing.

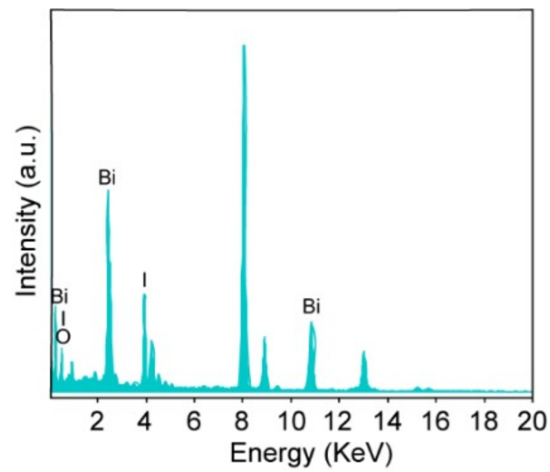

Figure S3. The energy-dispersive X-ray spectroscopy (EDS) of BiOI nanosheet.

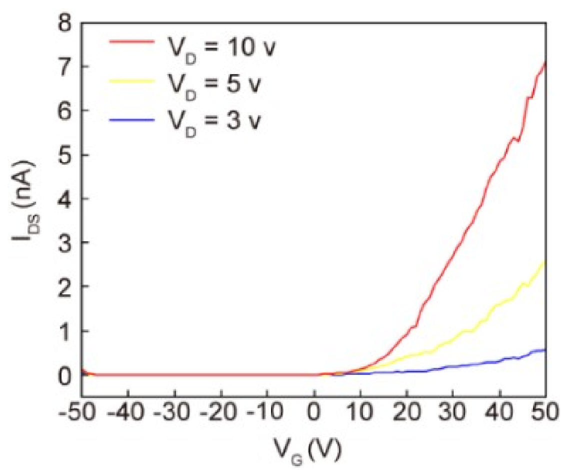

Figure S4. I_D-V_G curves of $BiOI/SiO_2$ transistors at different source-drain voltages, the n-type characteristics of BiOI were demonstrated.

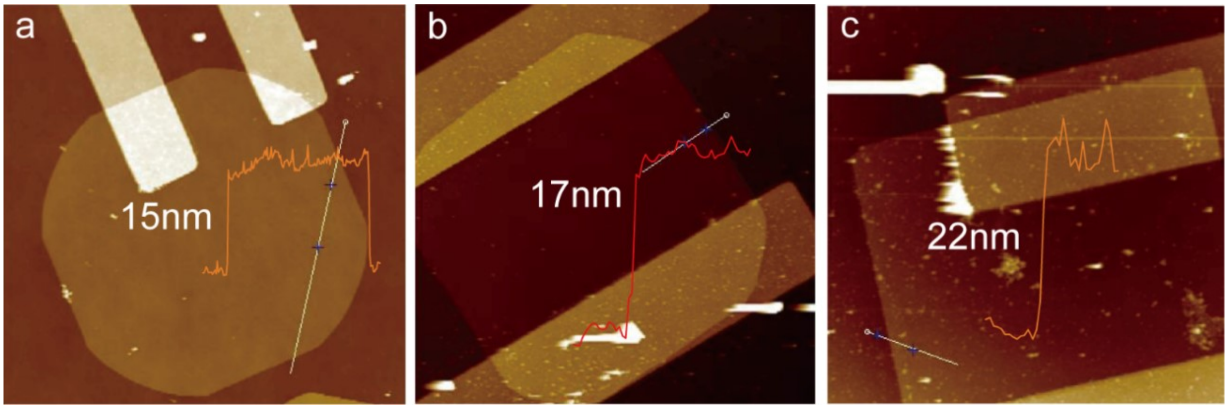

Figure S5. AFM images of BiOI devices of different thicknesses.

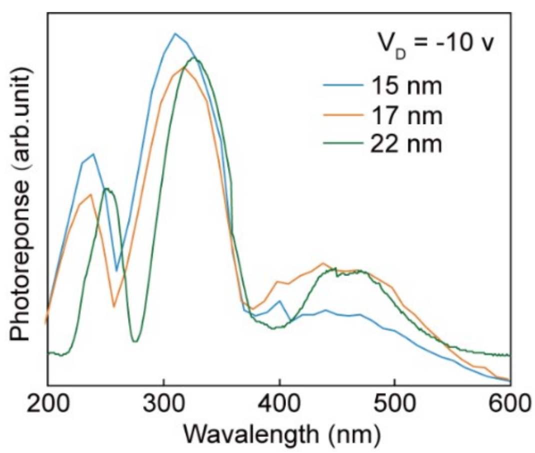

Figure S6. Optical response spectra of BiOI nanosheets with different thicknesses at 400 μW cm-2 power density under irradiation at different wavelengths.

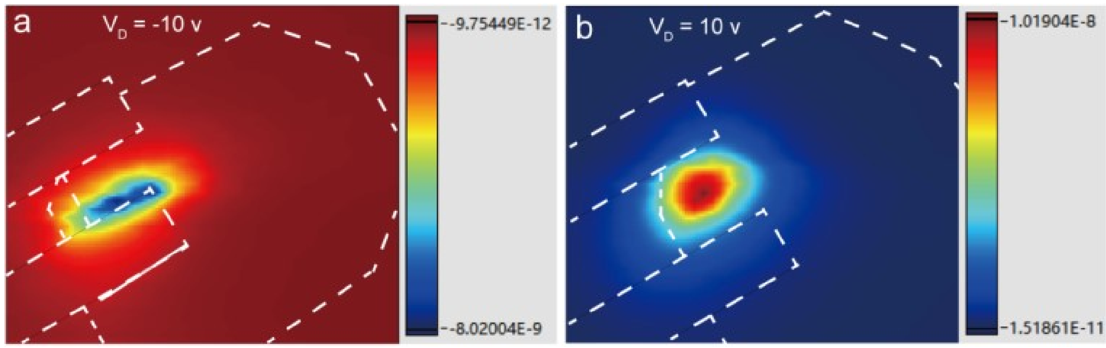

Figure S7. Scanning photocurrent mapping of the BiOI device under 405 nm laser illumination: (a) V_D = -10 V and(b) V_D = 10 V. The white dashed lines correspond to the outlines of BiOI and the electrodes.

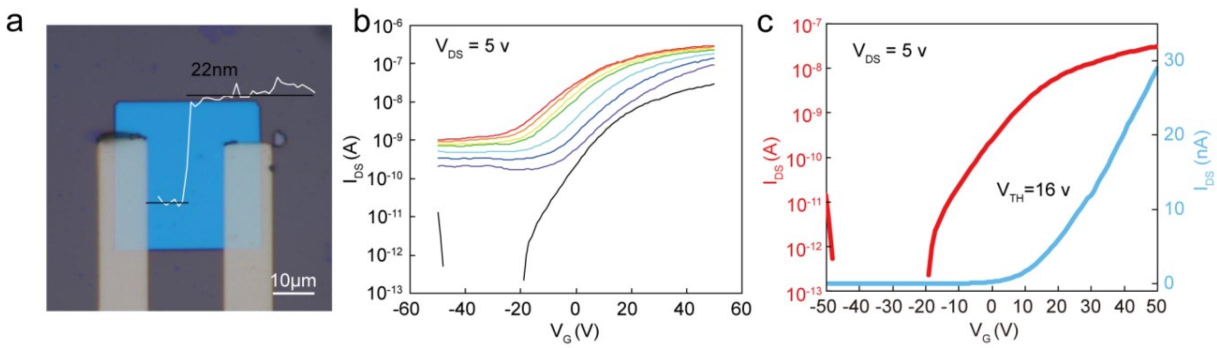

Figure S8. (a) Optical image of BiOI-based photodetectors. (b) The I_d-V_g curve of photocurrent controlled by SiO_2 as backgate. (c) Transfer curve of the BiOI FET, Vd = 5 V.

Table S1. Comparison of phototransistor performance based on the BiOI with other phototransistor.

Materials	R	D* (Jones)	EQE (%)	Response Time	λ(nm)	Growth method	Ref.
$NiPS_3$	126 mA W^{-1}	1.22×10^{12}	61	3.2/15.6 ms	254	CVD	1
BiOCl/ZnO	182.2 mA W^{-1}	—	—	29.23/11.20 s	350	hydrothermal	2
PbI_2	0.51 A W^{-1}	4.0×10^{10}	168.9	14.1/31 ms	275	solution	3
Zn_2GeO_4 Nanowire	5110 A W^{-1}	2.91×10^{11}	2.4×10^{6}	10/13 ms	260	CVD	4
GNA/ZnO	22.55 mA W^{-1}	—	9.35	2.5/11 s	300	Spin-coating	5
$Ga_2In_4S_9$	111.9 A W^{-1}	2.25×10^{11}	3.85×10^{4}	40/50 ms	360	CVD	6
$Sr_2Nb_3O_{10}$	1214 A W^{-1}	1.4×10^{14}	5.6×10^{5}	0.4/40 ms	270	liquid exfoliation	7
BiOI	26 mA W^{-1}	8.2×10^{11}	6.9	0.12/0.25 s	473	CVD	8
BiOI thin	43.5 mA W^{-1}	8.7×10^{10}	13	20.7/22.3 ms	405	CVD	9
BiOI	1048 mA W^{-1}	4.7×10^{12}	420	420/690 µs	310	molten salt	This work
	144 mA W^{-1}	6.46×10^{11}	144	—	532		

References

[1]J. Chu, F. Wang, L. Yin, L. Lei, C. Yan, F. Wang, Y. Wen, Z. Wang, C. Jiang, L. Feng, J. Xiong, Y. Li and J. He, Advanced Functional Materials, 2017, **27**, 1701342.

[2]F. Teng, W. Ouyang, Y. Li, L. Zheng and X. Fang, Small, 2017, **13**, 1700156.

[3]H. Xiao, T. Liang and M. Xu, Small, , DOI:10.1002/smll.201901767.

[4]X. Zhou, Q. Zhang, L. Gan, X. Li, H. Li, Y. Zhang, D. Golberg and T. Zhai, Advanced Functional Materials, 2015, **26**, 704–712.

[6]F. Wang, T. Gao, Q. Zhang, Z. Hu, B. Jin, L. Li, X. Zhou, H. Li, G. Van Tendeloo and T. Zhai, Advanced Materials, 2018, **31**, 1806306.

[7]S. Li, Y. Zhang, W. Yang, H. Liu and X. Fang, Advanced Materials, 2019, **32**, 1905443.

[8]W. Zeng, J. Li, L. Feng, H. Pan, X. Zhang, H. Sun and Z. Liu, Advanced Functional Materials, 2019, **29**, 1900129.

[9]Z. Sun, Y. Wang and B. Mei, Journal of Materials Chemistry C, 2023, **11**, 3805–3811.